Activation from Proton Irradiation of Zirconium Alloys

HIWA MOHAMMAD QADR[1,*], DYARI MUSTAFA MAMAND[2]

[1,2]University of Raparin, College of Science, Department of Physics, Sulaymaniyah, Iraq
Corresponding Author: Hiwa Mohammad Qadr (email: hiwa.physics@uor.edu.krd)

Abstract

An investigation into the irradiation of zirconium alloys with protons was carried out with respect to the capability for simulation of neutron damage as well as the associated activity which would accompany any suggested irradiation programme.Irradiations at 1, 3, 9 and 20 MeV were used to verify an activity modelling program which was found to be accurate in predicting the most active isotopes of Niobium from Zr(p,n)Nb direct reactions with zirconium but was less successful in replicating the relative gamma intensities of spectra recorded by a germanium detector of samples following irradiation.

Keywords: Zirconium alloys, Fortran, Activation, germanium detector

Introduction

Zirconium alloys offer excellent properties for structural components in fuel assemblies in reactor-cores because suitable structural, corrosion properties and low thermal neutron capture cross-section [1, 2]. Nonetheless, the phenomenon of irradiation induced growth is the one of the important life-limiting factors for these structural components. Irradiation induced growth is a dimensional change as a result of the introduction of line defects in the crystal structure via irradiation damage. Shrinkage occurs in the radial direction of the tubes and positive growth occurs in the axial direction due to the texture of the zirconium cladding [3-9].

Ion irradiation experiments allow control of ion energy, dose, dose rate and temperature which enables very reproducible and specific results making them desirable for studying irradiated micro-structure and property changes of a material in a shorter time period. However the evolution of irradiated microstructure is dependent upon a combination of damage rate and irradiation temperature and so damage cannot always be reproduced in a shortened time period just through increased displacement rate (dpa/s), although temperature shift relations have be created which allow for more correlation of one type of damage evolution from one irradiation environment to another using dose, dose rate and temperature. Ion beams are also generally cheaper to produce a given dose compared to neutron sources [10-15].

Accompanying irradiation is the resultant activity from satisfied Q-values of nuclear decays, although protons have less activity compared to heavier ions or neutrons for the same energy of incident particle, quantization of the dose and evaluation of the danger to persons involved in the handling of the samples is important for their safety and for agreement with legal dose limits. Being able to predict the magnitude of induced radiation and thus the percentage of allowable dose for the irradiation procedure would be useful as a preventative measure, consequently verification of a Fortran software [16, 17] able to do this will be carried out, the

program uses decay chains, Q-values for reactions and cross-sections with energy and its predictions will be verified by comparison to irradiated samples over a range of beam energies.

Activity simulation validation

Once all the data had been acquired from the HPG detector from each sample and energy, then comparisons between them could be made. The first comparison was made between pure zirconium (99.2%) and zircaloy-2 as can be seen in figure 1. This basic method was the first indication that zirconium could be the main cause of activation within the sample. To validate this, the characteristic gamma rays had to be identified with reactions and decays that were possible with zirconium.

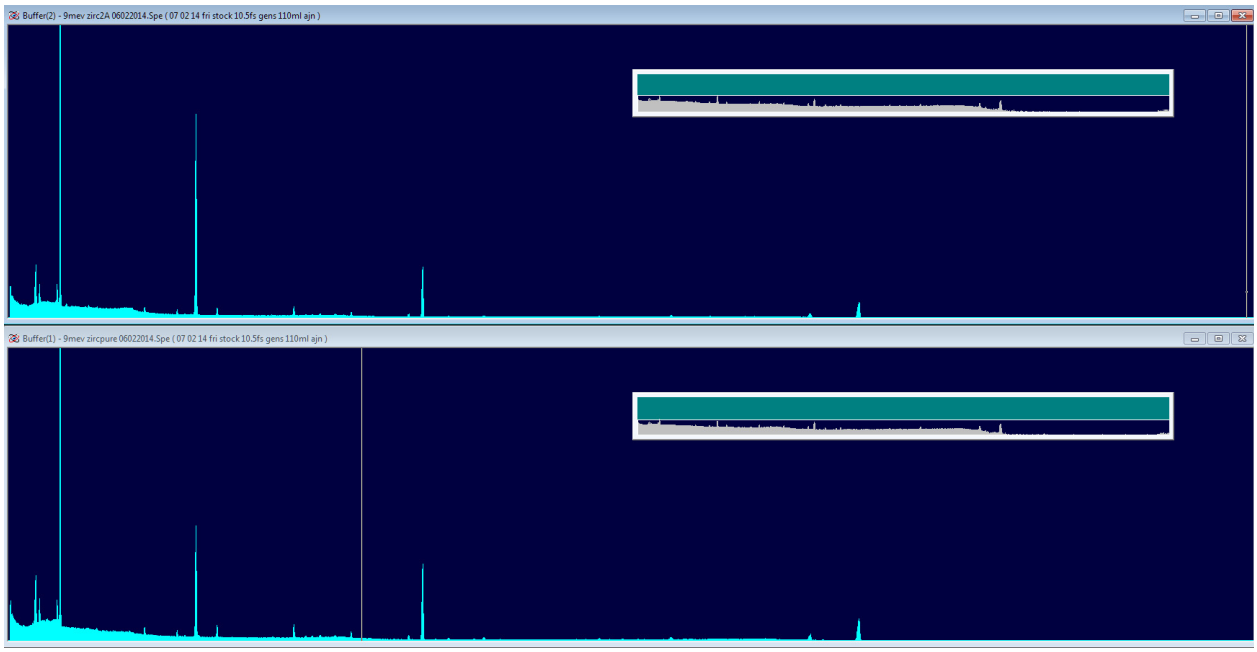

Figure 1. Comparison between gamma spectrum for zircaloy-2 (Top) and pure zirconium (bottom)

If the activity was mostly from isotopes of zirconium, then running simulation with 100% Zr should compare closely to experimental data. One of the simulations outputs shows the order of isotopes by highest activity. This turned out to be the most effective way of identifying the most important elements.

As seen in Table1, ^{90}Nb was simulated to be the most active with an activity of 1.59 x10^{6} Bq. The next step was to match up the characteristic gamma energies from the HPG detector with those of ^{90}Nb using the NNDC database [18]. NNDC gives the characteristic gamma rays for ^{90}Nb with their relative intensities [18, 19]. This was repeated for the most active elements on the list in Table1, until all of the peaks had been identified. This was done for each HPG detector measurement taken. Since the time between each irradiation and HPG measurement it was possible to run a simulation for the each measurement. The output in Table1was for 8463 safter 9 MeV irradiation for 600 s at 1.5 micro amps.

The next stage in the validation was to check if the formation of ^{90}Nb from Zr was possible. Uddin et al. [20]shows the possible reactions between a proton beam and isotopes of Zr and also can be shown that ^{90}Nb was caused by the ^{90}Zr absorbing a proton on the surface of the nucleus and then ejecting a neutron, ^{90}Zr(p; n)^{90}Nb [21]. From Uddin et al. [20] the threshold proton energy for this reaction is 6.97 MeV and therefore agrees with both simulation and

experimental data. The only other radionuclide that was identified from this measurement was ^{96}Nb, this was also simulated correctly as the second most active isotope. The ^{96}Zr(p; n) reaction was responsible for the formation of ^{96}Nb. The reaction had a threshold energy of 0.63 MeV, again lower than the ion beam energy used at 9 MeV.
Unfortunately, the simulation could not run for energies lower than 7 MeV, therefore comparisons between 1 and 3 MeV could not be made. If so then the simulation could have been run at energies lower than the threshold, to see if the reaction is no longer simulated and observed.
The other radionuclides simulated in Table 1 are also theoretically possible when compared to Uddin et al. [20], however they were not experimentally observed. This was most likely due to the low activities predicted together with significantly longer half lives. Measurements were taken over periods of days, of which by that time these radionuclides should have theoretically become more active however if present were below the background levels of the lab.

Table 1. Output for 8463 safter 9 MeV irradiation for 600 s at 1.5 micro amps

Element	Z	A	Bq
NB	41	90	0.00000159
NB	41	96	0.0000333
NB	41	95	0.00116
NB	41	97	0.0458
Y	39	87	0.458
Y	39	93	0.427
Y	39	91	0.364
NB	41	91	0.13
Y	39	88	3.65
Y	39	90	1.95
NB	41	94	2.62
Y	39	92	0.0309
ZR	40	95	0.0014
NB	41	92	0.000264
H	1	3	0.0000000314
ZR	40	93	0.00000000494

The second most active radionuclide at this point in time was ^{96}Nb after which had a longer half of 23.35 than the most active ^{90}Nb with a half life of 14.6 hours. Therefore after a certain time ^{90}Nb should become less active than ^{96}Nb. The time in which this takes to happen can be analytically solved by equating [21]:

$$A_0 e^{-t\lambda t} = A_0 e^{-t\lambda t} \quad (1)$$

$$ln\left(\frac{A_0}{A_0}\right)\frac{1}{\lambda_{90_{Nb}} - \lambda_{96_{Nb}}} = t \quad (2)$$

Inserting values for $^{90Nb}A_0$ and $^{96Nb}A_0$ from Table1 and then using half-lives from reference [20] with $\frac{ln2}{t_{1/2}}$to calculate the decay constants which gave a time of 3 days and 16 hours. A simulation was run for 2 days and 21 hours after the simulation previously mentioned and

^{90}Nb was still more active as expected. The next simulation was run after 3 days and 20 hours from the first simulation and as expected ^{96}Nb had become more active than ^{90}Nb.
The next stage in the comparison was to compare the 9 MeV spectrums with that of 20MeV to see if there is a difference in the simulated and observed radionuclides. Figure 2 shows the comparison between 9 MeV and 20 MeV spectrums within maestro, the only difference arises from a 909.14 keV characteristic peak. To determine what this element was the simulation was run at 20 MeV and the elements by most active were then analyzed.
Again, ^{90}Nb was the most active; however, the second most active element was ^{89}Zr which was not simulated at 9 MeV at all. Uddin et al. shows the possible reaction that causes ^{89}Zr (characteristic peak of 909.14 keV) to be, ^{90}Zr(p; d) .i.e. a ^{90}Zr nucleus absorbs a proton at its surface and ejects a deuteron. The threshold energy for this reaction is 9.85 MeV which agrees with experimental and simulation results[20].

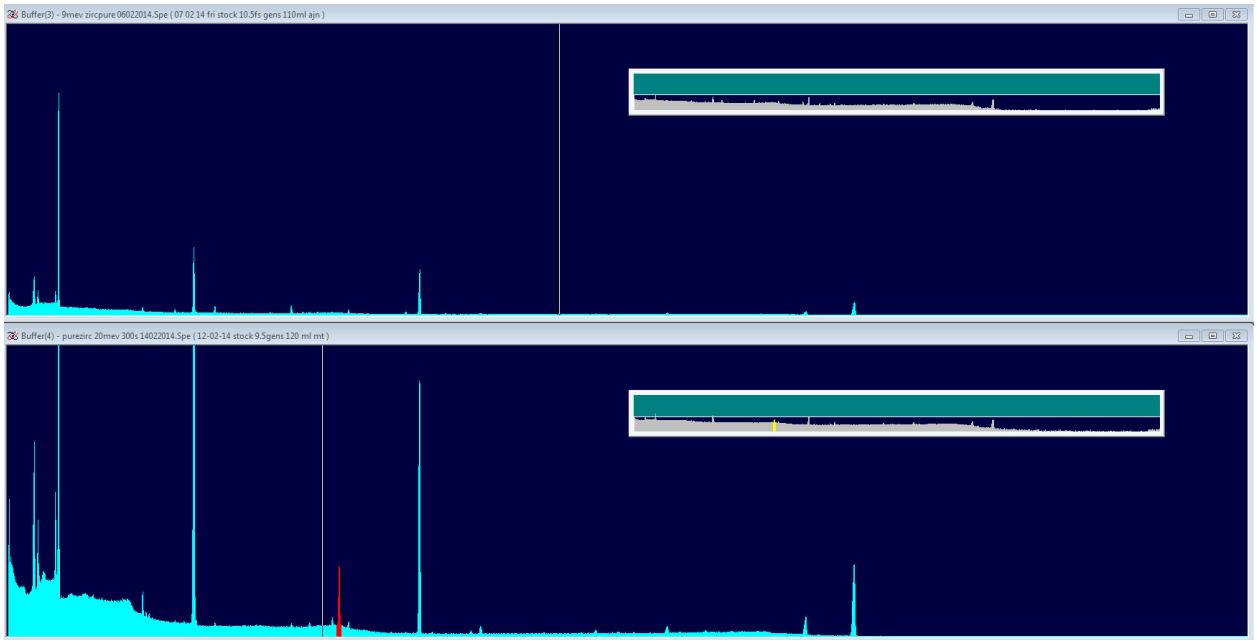

Figure 2. Comparison between 9 MeV and 20 MeV

Result and Discussion

Total Activity at different Irradiation Energies

Irradiation was performed on a sample of 99.2% pure zirconium at different energies: 1 MeV, 3 MeV, 9 MeV and 20 MeV. Measurements of the overall activity were taken using the germanium detector about 1 hour after each irradiation. In figure 3 there is a plot of the overall activity against irradiation energy. The data seem to be showing a linear trend. More energy means that each irradiated particle has on average more energy and therefore it is able to deposit more energy during interaction with matter. This is not true for protons at low energies because their charge will `force' the interaction and they will not make it through the material. This means that by lowering the energy of a proton beam it is possible to deliver more damage nearthe surface where the majority of the protons stop. However, using the Bragg peak todamage material is very risky as this can promote several reactions between protons andneutrons to give out hydrogen. Hydrogen embrittlement is a phenomenon that wouldnot occur with neutrons as much as it would with protons. It is therefore imperative thatthe Bragg peak is avoided if the ultimate result of these studies has to be the simulation of neutron damage.

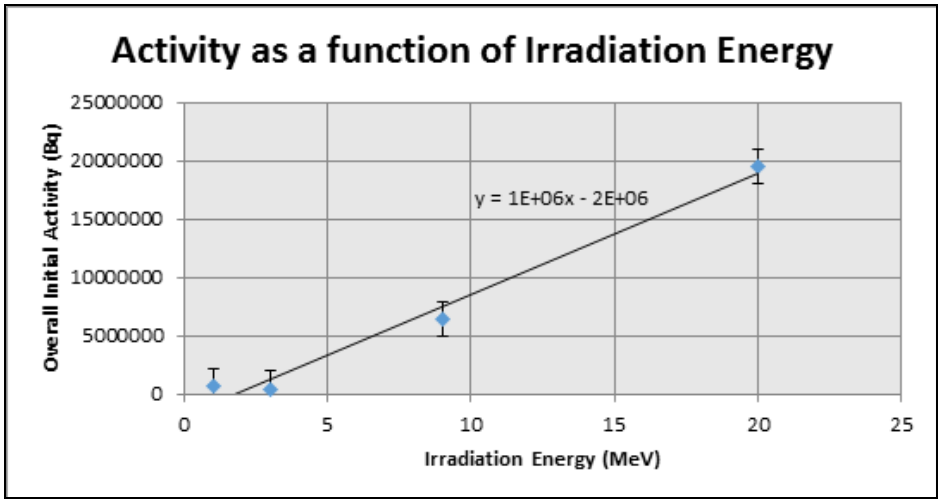

Figure 3. Overall activity for different irradiation energies

Measuring the Overall activity

The Fortransoftware was run in order to simulate the same irradiation conditions of the 9 MeV pure zirconium sample and its total activity was plotted against time. The activity starts being measured from when the beam stops. In the same diagram the activity of the real sample was plotted against time for comparison. The activity was measure with the germanium detector five times over three days. In order to make the two curves more comparable. Also, 5 points were highlighted on the Fortrancurve corresponding to the points in time were the germanium measurements were taken to be able to spot the difference more easily as shown in figure 4.

As it can be seen from the graph, the activity predicted by the model is higher than the one that was measured experimentally. This might be due to imperfections in the irradiation machinery that lead to more surface being irradiated, imperfections within the specimen or to imperfections in the Fortran software. Further studies could be conducted to investigate this further.The error was calculated by multiplying each individual peak area-error by the standard deviation and it is therefore proportional to the area, the counts and so the activity. No error bars were fitted on the Fortran plot as the code predicts the theoretical activity.

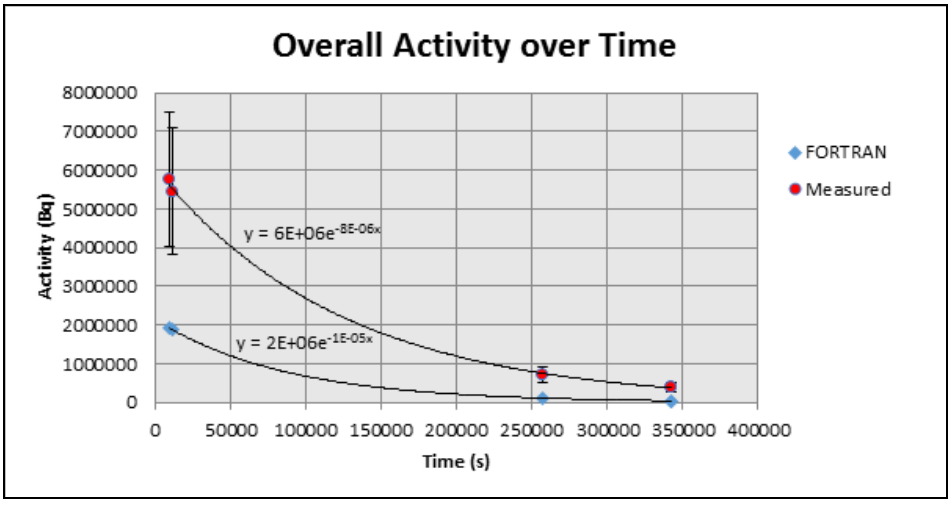

Figure 4. Comparison between Fortran and HP-Ge detector total activity

Individual Isotope Activities

When pure zirconium is irradiated with a proton beam, various isotopes of Niobium are formed. The most common Niobium isotopes are ^{90}Nb, ^{96}Nb and Nb^{97}. ^{90}Nb and ^{96}Nb alone are responsible for over 97% of the total activity of the sample in the first few days. Nb^{97} and a few Y isotopes follow along and are pivotal in the activation later on. Fortran lists, along with the total activity, a top-ten of the most active elements in increasing order. The only two isotopes that were detected by the germanium detector and identified through maestro are ^{90}Nb and ^{96}Nb. By isolating the peaks, it was possible to identify what peaks belong to what elements and the total number of counts for each Niobium isotope was calculated. Finally, the Fortran activities were compared with the measured ones in the figure 5.

There is discrepancy between the results shown in figure 4 and the ones in figure 5. This might be due to the fact that when the data were originally collected from maestro and copied on to spreadsheets, two of the largest peaks belonging to each one of the two isotopes in question were accidentally neglected. Both ^{90}Nb and ^{96}Nb happen to have high relative intensity peaks out of the part of the spectrum that maestro defaults for the user to view. Maestro `hides' some of the spectrum because it assumes that the user is not interested in viewing it. In the case of ^{90}Nb and ^{96}Nb there is such an interest.

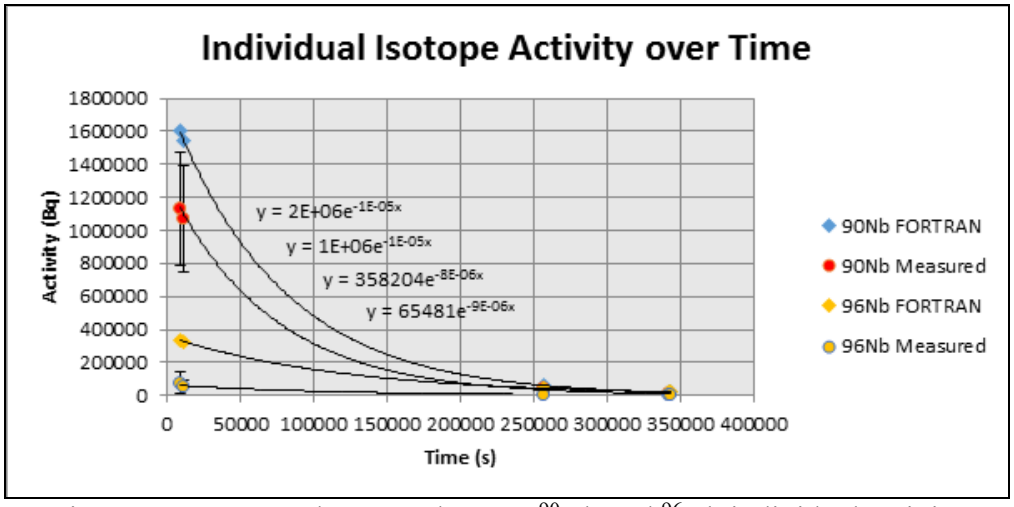

Figure 5. Fortran and HP-Ge detector ^{90}Nb and ^{96}Nb individual activity

Different Irradiation Energies

The total activity of the 9 MeV pure zirconium sample and the 20 MeV pure zirconium sample was measured over time with the germanium detector. Unfortunately, measurements for the activity of the 20 MeV sample were only made in two different days, adding considerable error to the results that was calculated to be 20% and it is the average difference between background measurements.However, it was possible to plot the decay equation for both decays in figure 6 and calculate their half-life, equation 3 for 20 MeV and 4 for 9 MeV:

$$t_{1/2} = \frac{ln2}{\lambda} = \frac{0.693}{9 \times 10^{-6}} = 77016.35s \approx 21.4h \quad (3)$$

$$t_{1/2} = \frac{ln2}{\lambda} = \frac{0.693}{6 \times 10^{-6}} = 115524.53s \approx 32.1h \quad (4)$$

After irradiating pure zirconium with a much higher energy of 20 MeV, one would expect the activity to be higher but with the same half-life. When the particle energy (in this case, the proton energy) increases, new reactions are possible, and new states that were inaccessible at lower energies 9 MeV are now accessible. At a different energy, all cross-sections for all

reactions change and after the beam is switched off new isotopes form, emitting radioactivity at a different rate and decaying at a different rate. The difference might also be due to the fact that only two measurements were taken for the 20 MeV sample. Future studies could be conducted to investigate this phenomenon further and activity should be taken at least once per day once the samples are safe to handle.

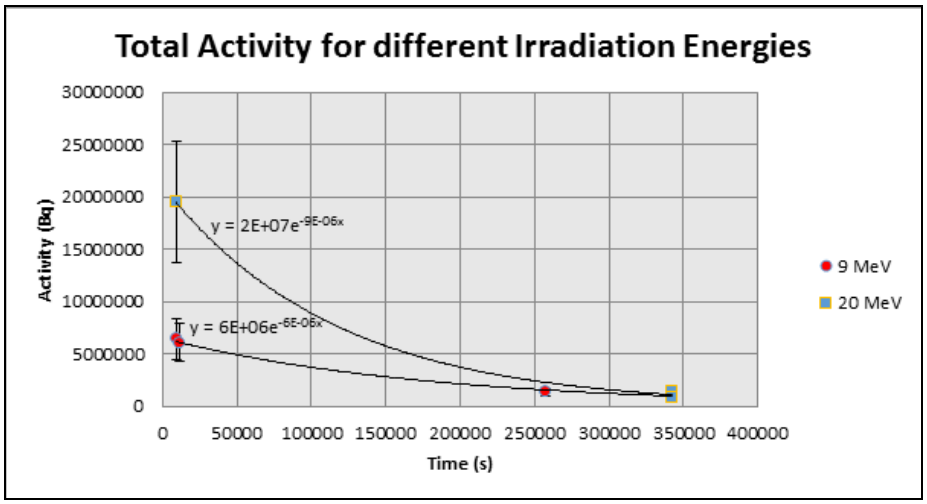

Figure 6. 9 MeV and 20 MeV decays compared

Conclusion

The simulation was a useful tool in highlighting the main radionuclides that were formed during the irradiation of the ziracloy-2 and pure zirconium samples. However, as for its use for the activity simulation in its current form should not be used for this purpose. This was because the simulation significantly underestimated the activity when compared to the actual activity measured with the HPG detector. The two main reasons identified to be the cause of this underestimate. Firstly, the simulation did not take into account electron and positron annihilation. Secondly, the simulation did not have cross section data for Zr below around 7 MeV, this means that once the proton reached this energy within the sample then no more activity could be simulated and therefore not taken into account into the overall activity. Therefore, suggested improvements to code would be to add cross section data for missing energies to the existing databases. In addition, the positron and electron annihilation should be taken into account. Another important improvement would be the addition of ^{90}Nb gamma spectrums as this one of the main radionuclides produced.

References

[1] X.B. Liu, R.S. Chen, E.H. Han, *Effects of ageing treatment on microstructures and properties of Mg–Gd–Y–Zr alloys with and without Zn additions*, Journal of Alloys and Compounds 465(1-2) (**2008**) 232-238.

[2] H.M. Qadr, *Effect of ion irradiation on the hardness properties of Zirconium alloy*, Annals of the University of Craiova, Physics 29 (**2019**) 68-76.

[3] M. Topping, A. Harte, T. Ungár, C.P. Race, S. Dumbill, P. Frankel, M. Preuss, *The effect of irradiation temperature on damage structures in proton-irradiated zirconium alloys*, Journal of Nuclear Materials 514 (**2019**) 358-367.

[4] M.Q. Hiwa, *The use of the MCNP Code for Radiation Damage Calculations*, Mathematical Physics and Computer Modeling 24(1) (**2021**). https://doi.org/10.15688/mpcm.jvolsu.2021.1.5

[5] M.Q. Hiwa, M.H. Ari, *Investigation of long and short term irradiation hardening of P91 and P92 ferritic/martensitic steels*, Problems of Atomic Science and Technology. Series:Thermonuclear Fusion 42(2) (**2019**) 81-88.

[6] I.N. Qader, H.M. Qadr, P.H. Ali, *Calculation of Lattice Thermal Conductivity for Si Fishbone Nanowire Using Modified Callaway Model*, Semiconductors 55(12) (**2021**) 960-967. 10.1134/S1063782621070137

[7] H.M. Qadr, *Effect of ion irradiation on the mechanical properties of high and low copper*, Atom Indonesia 46(1) (**2020**) 47-51. https://doi.org/10.17146/aij.2020.923

[8] H.M. Qadr, *A molecular dynamics calculation to cascade damage processes*, The Annals of "Dunarea de Jos" University of Galati. Fascicle IX, Metallurgy and Materials Science 43(4) (**2020**) 13-16. https://doi.org/10.35219/mms.2020.4.02

[9] H.M. Qadr, *A Molecular Dynamics Study of Temperature Dependence of the Primary State of Cascade Damage Processes*, Russian Journal of Non-Ferrous Metals 62(5) (**2021**) 561-567. https://doi.org/10.3103/S1067821221050096

[10] H.M. Qadr, A.M. Hamad, *MECHANICAL PROPERTIES OF FERRITIC MARTENSTIC STEELS: A REVIEW*, Scientific Bulletin of'Valahia'University. Materials & Mechanics 17(16) (**2019**).
[11] H.M. Qadr, D. Mamand, *A Review on DPA for computing radiation damage simulation*, Journal of Physical Chemistry and Functional Materials 5(1) (**2022**) 30-36.

[12] H.M. Qadr, D.M. Mamand, *Molecular Structure and Density Functional Theory Investigation Corrosion Inhibitors of Some Oxadiazoles*, Journal of Bio- and Tribo-Corrosion 7(4) (**2021**) 140. https://doi.org/10.1007/s40735-021-00566-9

[13] M. Li, M.A. Kirk, P.M. Baldo, D. Xu, B.D. Wirth, *Study of defect evolution by TEM with in situ ion irradiation and coordinated modeling*, Philosophical Magazine 92(16) (**2012**) 2048-2078.

[14] H.M. Qadr, *Pressure Effects on Stopping Power of Alpha Particles in Argon Gas*, Physics of Particles and Nuclei Letters 18(2) (**2021**) 185-189. https://doi.org/10.1134/S1547477121020151

[15] H.M. Qadr, *Experimental Study of the Pressure Effects on Stopping Power for Alpha Particles in Air*, Gazi University Journal of Science (**2022**) 272-279.

[16] U. Ellwanger, J.F. Gunion, C. Hugonie, *NMHDECAY: A Fortran code for the Higgs masses, couplings and decay widths in the NMSSM*, Journal of High Energy Physics 2005(02) (**2005**) 066.

[17] H.M. Qadr, *Radiation damage and dpa in iron using mcnp5*, European Journal of Materials Science and Engineering 5(3) (**2020**) 109-114.

[18] NNDC, National Nuclear Data Center. https://www.nndc.bnl.gov/nudat3/.

[19] B. Pritychenko, A.A. Sonzogni, D.F. Winchell, V.V. Zerkin, R. Arcilla, T.W. Burrows, C.L. Dunford, M.W. Herman, V. McLane, P. Obložinský, *Nuclear reaction and structure data services of the National Nuclear Data Center*, Annals of Nuclear Energy 33(4) (**2006**) 390-399.

[20] M.S. Uddin, M.U. Khandaker, K.S. Kim, Y.S. Lee, M.W. Lee, G.N. Kim, *Excitation functions of the proton induced nuclear reactions on natural zirconium*, Nuclear Instruments and Methods in Physics Research Section B: Beam Interactions with Materials and Atoms 266(1) (**2008**) 13-20.

[21] K.S. Krane, *Introductory nuclear physics*, John Wiley & Sons1991.